Spiral waves in a coupled network of sine-circle maps

Sung-Jae Woo,[1] Jysoo Lee,[1,2] and Kyoung J. Lee[1,*]
[1]*National Creative Research Initiative Center for Neuro-dynamics and Department of Physics, Korea University, Seoul 136-701, Korea*
[2]*Supercomputing Center, Korea Institute of Science and Technology Information, Yusong-Gu, Eoeun-Dong 52, Daejon 305-806, Korea*

(Received 30 October 2002; revised manuscript received 11 March 2003; published 14 July 2003)

A coupled two-dimensional lattice of sine-circle maps is investigated numerically as a simple model for coupled network of nonlinear oscillators under a spatially uniform, temporally periodic, external forcing. Various patterns, including quasiperiodic spiral waves, periodic, banded spiral waves in several different polygonal shapes, and domain patterns, are observed. The banded spiral waves and domain patterns match well with the results of earlier experimental studies. Several transitions are analyzed. Among others, the source-sink transition of a quasiperiodic spiral wave and the cascade of ''side-doubling'' bifurcations of polygonal spiral waves are of great interest.

DOI: 10.1103/PhysRevE.68.016208 PACS number(s): 05.45.Xt, 82.40.Ck, 05.70.Ln, 47.54.+r

Nonlinear oscillators driven by a small amplitude external forcing can either exhibit quasiperiodic (unlocked) or periodic (locked) oscillations, depending on the values of the forcing amplitude and frequency [1,2]. For the frequency-locked case, the oscillator is detuned from its natural frequency and oscillates at a rational multiple of the external driving frequency. Systems exhibiting such a phenomenon are extensively studied over the past few decades for having a universal structure of frequency-locked states based on the Farey construction and for exhibiting a generic route to the low-dimensional chaos [1].

As recent experimental and theoretical studies have revealed, the phenomenon of frequency locking also arises in spatially extended systems under an external forcing [3–11]. A variety of interesting patterns can be formed in these systems due to the degree of freedom in space. Petrov *et al.* addressed this issue for the first time in an experiment employing a light sensitive Belousov-Zhabotinsky (BZ) reaction-diffusion system [5]. The system was brought to an oscillatory regime and perturbed in a time-periodic manner using light. Several interesting spatial patterns, including fronts and labyrinth of 2:1 mode locking, irregular domain pattern of 3:1 mode locking, and ''bubble patterns'' of 3:2 mode locking, had emerged.

Following these experimental observations, several model systems were investigated to elucidate the underlying pattern forming mechanism [12,9,7,8,11]. Among others, the numerical and theoretical analyses done by Elphick *et al.* [9] on a generic complex Ginzburg-Landau (CGL) equation is quite notable. They have shown that there can be different types of fronts and front instabilities in frequency-locked regime, similar to the front instabilities mediating static labyrinth patterns and traveling (spiral) waves in a bistable system [13–15]. So far, similar patterns are also produced in several different model reaction-diffusion systems under an external forcing [7,12,9,8]. Thus, there seem to be some universal rules, concerning the types of patterns and bifurcations arising in a spatially extended network of nonlinear oscillators under an external forcing.

Along this venue of thought, we have studied patterns arising in a coupled map lattice (CML) of sine-circle maps. The phenomenon of frequency locking is, perhaps, best understood by the sine-circle map for its simplicity and computational efficiency [1]. Therefore, it seems rather natural to use a CML of sine-circle maps for investigating generic properties of the patterns arising in a coupled network of nonlinear oscillators under an external forcing. Although various CMLs (especially, of the logistic maps) have been investigated a lot in the past [16–18], they were mostly concerned about spatiotemporal chaos.

The CML of sine-circle maps is given by

$$x_{ij}^{(t+1)} = f(x_{ij}^{(t)}) + \epsilon \sum_{l,m} [g(x_{lm}^{(t)}) - g(x_{ij}^{(t)})] (\mathrm{mod} 1), \quad (1)$$

where $f(x) = x + \Omega + (K/2\pi)\sin 2\pi x$ and $g(x) = -\sin(2\pi x)$. The variable x_{ij} is the oscillation phase of the square lattice site (i,j). The $f(x)$ is the sine-circle map and the following summation term represents the interactions with four nearest neighbors. Ω, K, and ϵ are the bare rotation number, the strength of the forcing, and the coupling constant, respectively. Square lattice of 128×128 grids is used unless otherwise mentioned. No-flux boundary condition is used throughout the paper.

The sine-circle map $f(x)$ can produce a variety of different mode-locked states (resonant bands) based on the parameter values of K and Ω. Our current investigation is mainly focused on the 2:5 resonant band as a typical example of n:m resonances (n and m are positive integers) and its vicinity, and this is in a good contrast with the earlier model studies [12,9,7,8,11] that were mainly focused on elementary n:1 resonant bands (i.e., $m=1$ cases). Figure 1 illustrates three different types of patterns observed within or near the 2:5 resonant band. The smooth spiral wave of Fig. 1(a) has a quasiperiodic local dynamics as its first return map of a local time series well illustrates. On the other hand, the square-shaped spiral wave of Fig. 1(b) exhibits a periodic local dynamics as the map repeatedly visits the five points (1–5). The domain pattern shown in Fig. 1(c) also has a periodic local dynamics. Unlike the rotating quasiperiodic spiral

*Electronic address: kyoung@nld.korea.ac.kr

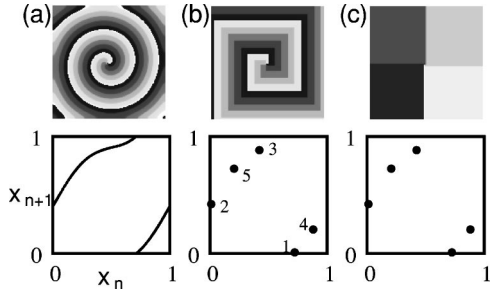

FIG. 1. Patterns observed in a sine-circle CML and the corresponding first return maps of a local time series: (a) regular, quasiperiodic spiral wave ($\Omega = 0.403\,87$), (b) square-shaped, periodic spiral wave ($\Omega = 0.404\,13$), and (c) periodically oscillating domain ($\Omega = 0.406\,30$). A stack of four line segments with different phase values is used as an initial condition. Throughout this paper, the values of K and ϵ are fixed at 0.75 and 0.002, respectively.

wave, the square-shaped periodic spiral wave and the domain pattern are both standing waves and are sensitive to the initial condition. For example, the patterns in Figs. 1(b) and 1(c) are obtained as the value of Ω is gradually increased, in particular, from the regular spiral wave state shown in Fig. 1(a).

The transition from the quasiperiodic spiral wave of Fig. 1(a) to the periodic spiral wave of Fig. 1(b) can be characterized in two different ways. As the value of Ω increases, the quasiperiodic spiral wave starts to bend acquiring a square symmetry [see Fig. 2(a)]. When the value of Ω increases further, the bent spiral wave becomes more flattened and eventually becomes the square-shaped spiral wave of Fig. 1(b). While this shape transformation takes place, the distribution of the phase variable x also changes dramatically from a dispersed spectrum [Fig. 2(b)] to a state with five localized peaks [Fig. 2(d)] via an intermediate state [Fig. 2(c)]. The emergence of the sharp peaks in the phase angle distribution reflects the fact that steep phase fronts have been established in space, separating the five domains of different phases. The finite width of the peaks in the phase distribution

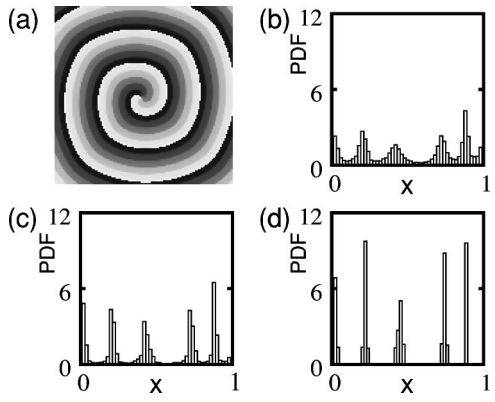

FIG. 2. Quasiperiodic to periodic spiral wave transition: (a) quasiperiodic spiral wave having a square symmetry ($\Omega = 0.404\,10$), (b) phase angle probability density function (PDF) of a quasiperiodic spiral wave, (c) PDF for (a), and (d) PDF for a periodic spiral wave. Ω is (b) 0.403 50, (c) 0.404 10, and (d) 0.404 13, respectively.

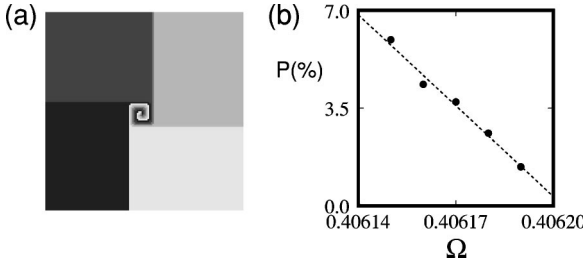

FIG. 3. Transition of a square-shaped spiral wave to a domain pattern: (a) an intermediate state exhibiting both a square-shaped spiral (the middle part) and a domain state (the outer part) [$\Omega = 0.406\,19$] and (b) proportion of the spiral domain P vs Ω.

of Fig. 2(d), nevertheless, indicates that the phase fronts have a finite width. The 5-phase spiral wave is the reminiscent of the 2:5 resonant band. Since the spiral shape changes continuously and the widths of the phase fronts narrow down gradually, one may conclude that the transition of the quasiperiodic spiral wave to the periodic spiral wave is continuous.

The square-shaped spiral wave further transforms to the domain pattern of Fig. 1(c) as the parameter Ω approaches the right end of the 2:5 resonant band: The spiral first dilates from the boundary and opens up as shown in Fig. 3(a). This process takes place in a continuous manner as shown in Fig. 3(b): The central region occupied by the square-shaped spiral shrinks rapidly but continuously to zero. The domain pattern persists until the system reenters a quasiperiodic regime upon increasing the value of Ω.

In addition to the square-shaped spiral wave and the domain pattern, various polygonal spiral waves are also found within the same 2:5 resonant band (see Fig. 4). In other words, multiple attractors (spirals) can coexist even for a fixed value of Ω [see Fig. 4(e)]. Thus, the final state being selected depends on the initial condition. For example, the

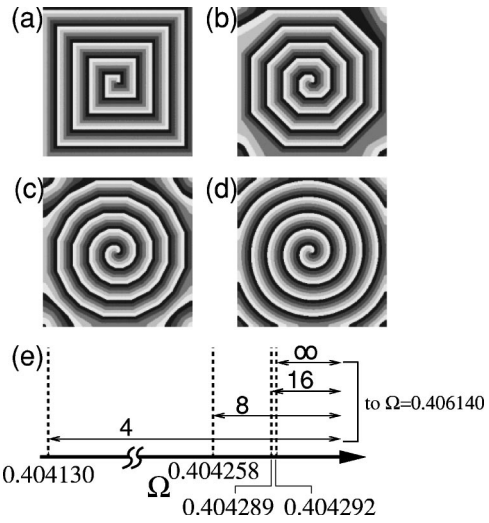

FIG. 4. Periodic spiral waves having (a) 4 sides, (b) 8 sides, (c) 16 sides, and (d) an infinite number of sides. (e) Phase diagram of polygonal spiral waves. Ω is 0.404 13, 0.404 28, 0.404 29, and 0.4043 [from (a) to (d)]. The polygonal spirals are, in general, not equilateral. A square lattice of 256×256 grids is used.

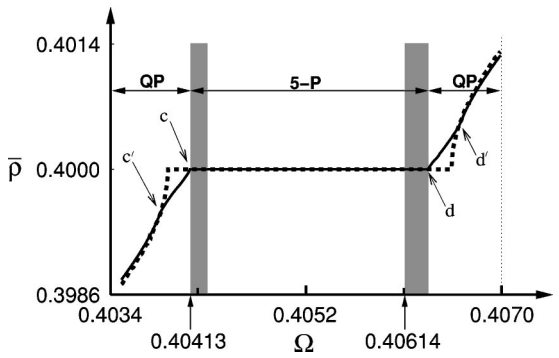

FIG. 5. Phase diagram drawn on the spatially averaged winding number $\bar{\rho}$ of the sine-circle CML (solid line). The winding number ρ of a single sine-circle map is overlaid (dashed line). ''QP'' and ''5-P'' stand for the quasiperiodic spiral wave and the 5-phase periodic spiral wave, respectively. The domain patterns are stable for the shaded regions only. Polygonal spirals of Fig. 4 also coexist in the 5-P region, but are not shown in this diagram for clarity; the detailed phase diagram of the polygonal spirals is given in Fig. 4(e).

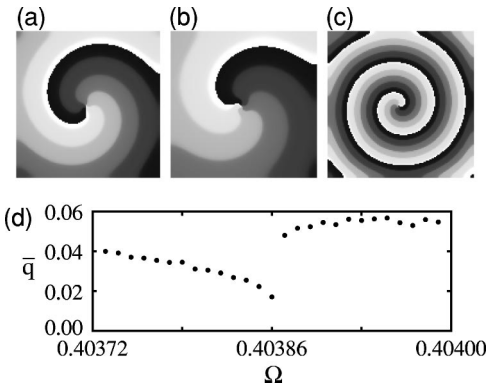

FIG. 6. Spiral to antispiral transition: (a) quasiperiodic spiral wave having a source at its core ($\Omega = 0.403\,85$), (b) a mixed spiral wave state ($\Omega = 0.40386$), and (c) quasiperiodic spiral wave having a sink at its core ($\Omega = 0.40387$). (d) Plots an averaged (Fourier power weighted) wave number $\bar{q}$ vs Ω.

regular, octagonal spiral wave of Fig. 4(b) is obtained by decreasing the value of Ω from the smooth, banded spiral wave of Fig. 4(d). But if one had used the square-shaped spiral wave of Fig. 4(a) as an initial condition and increased the value of Ω, the final state would have been the square-shaped spiral wave itself since it is stable there as well. Most significant of all, higher-order polygonal spiral waves [e,g., 16-faced spiral wave as shown in Fig. 4(c) or 24-faced spiral wave (not shown)] are also observed within the 2:5 resonant band. In fact, there seems to be a cascade of side-doubling bifurcations of polygonal spiral waves in an increasing sequence of Ω. The maximum number of faces that the polygonal spiral can have, or rather that we can identify, seems just limited by the system size.

We note that spatial period-doubling bifurcations have attracted much attention in recent years in relation to complex periodic spiral waves [19–22] and to superlattice standing waves [23,24]. The side-doubling transition of polygonal spiral waves, yet, is a different type of spatial period-doubling cascade. Our preliminary investigation suggests that the stability of a particular polygonal spiral wave is closely related with the stability of a planar wave traveling in a particular direction on the square lattice. For example, the octagonal spiral wave is stable for the Ω range for which the corresponding planar wave is stable in the direction of (1,0) as well as in the direction of (1,1).

Figure 5 plots the spatially averaged winding number $\bar{\rho}$ of the sine-circle CML as a function of Ω. The regions of stability for different types of patterns are illustrated on top of it. Several features are notable here. First of all, the domain patterns of the type shown in Fig. 1(c) are found to be stable not only near the right end but also near the left end of the resonant band (shaded regions): In a decreasing sequence of Ω, an initial spiral wave becomes a domain pattern entering the left end (shaded region) of the resonant band. Second, stable square-shaped spiral waves are found in the whole range of the resonant band (from the point c to d); in a decreasing sequence of Ω, an initial quasiperiodic spiral wave becomes a square-shaped spiral at point d. Then, the square-shaped spiral wave persists until it becomes a domain pattern entering the shaded area on the left. Third, the overall shape of $\bar{\rho}$ is nearly identical to the winding number ρ of a single (uncoupled) sine-circle map, except for the intervals $c'-c$ and $d'-d$.

The two points c' and d', at which $\bar{\rho}$ starts deviating from ρ, are significant since an interesting source-sink transition arises there. Figure 6 depicts this transition. The regular quasiperiodic spiral wave shown in Fig. 6(a) rotates in the counterclockwise direction generating an outwardly moving wave train (i.e., the spiral core acts as a source) [25]. When the parameter Ω is increased beyond c', the regular spiral transforms into an antispiral [Fig. 6(c)] via the intermediate state [Fig. 6(b)]. The antispiral has chirality opposite to the regular spiral, but rotates in the counterclockwise direction as in the regular spiral wave of Fig. 6(a). Consequently, the core of the antispiral is a sink. The intermediate state is a mixed state of an inwardly rotating spiral (the small area around the core) and an outwardly rotating spiral (the remaining outer part). As the parameter increases, the area being occupied by the antispiral grows at the expense of the regular spiral. Figure 6(d) quantifies this transition with the averaged wave number $\bar{q}$; $\bar{q}$ gradually decays approaching the critical point c' from the left and then rapidly increases beyond c'. Within the resolution of our current numerical simulations, the transition is continuous. As Fig. 5 illustrates, the average frequency of the antispiral wave (i.e., $\bar{\rho}$) is smaller than that of the bulk medium ρ, while the regular spiral wave has a slightly higher frequency than that of the bulk medium. The source-sink transition arises once again at point d'.

In summary, as a simple model system of oscillatory media under an external periodic forcing, a coupled network of sine-circle maps is investigated numerically. Stable periodic and quasiperiodic spiral waves are shown to exist in a sine-circle CML. Some important characteristics of the patterns observed in the BZ experimental system [5–7,10] and the continuous CGL equations studied earlier [12,9,7,8,11] are well captured in this simple model. In particular, the peri-

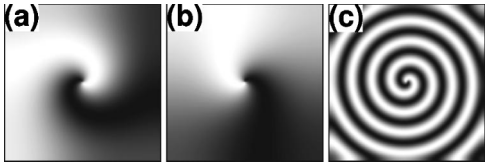

FIG. 7. Source-sink transition observed in a numerical simulation of CGL equation: $\partial_t A = A - (1+i\beta)|A|^2 A + (1+i\alpha)\nabla^2 A$. The outwardly rotating spiral wave (source) in (a) is transformed into the inwardly rotating spiral wave (sink) in (c) as α continuously increases: α is -2.0, -0.6, -0.2 from (a) to (c). β is fixed to be -1. Each frame is a gray scale image of Re(A), and has a size of 256×256 grids.

odic, banded spirals and domain patterns seem to be universal features of a driven network of nonlinear oscillators in resonance. There is, however, a subtle difference between the banded spiral waves in continuous systems and those of the discrete system. Above all, none of the previous studies on spiral waves, which were carried out in a continuous medium, reported a polygonal spiral. In other words, the polygonal spirals are believed to be a unique property pertaining to a discrete system.

Spiral waves having a sink at the core (antispirals) were first discovered by Vanag and Epstein in a recent experiment on an excitable BZ reaction-diffusion system [26,27]. Here, we have shown that an antispiral wave exists in a discrete model system of sine-circle CML. More recently, as an effort to understand the underlying mechanism of the antispiral, we have also investigated a two-dimensional complex Ginzburg-Landau equation to confirm the existence of the same transition (see Fig. 7) [29]. Thus, judging from the fact that similar transitions are observed in two quite different model systems (one is discrete, while the other is continuous), as well as in the experiment done by Vanag and Epstein, the spiral to antispiral wave transition seems to be a generic property of any spiral wave forming system.

Finally, we indicate that the observed phenomena are not just limited to the 2:5 resonant band but seem to be general. Several other resonant bands that we have checked have a shape of $\overline{\rho}$ that is similar to the one shown in Fig. 5, i.e., the transition points c' and d' also exist for them as well. Besides, quasiperiodic spiral waves and periodic, banded spiral waves are also popularly observed within (or near) other resonant bands.

We thank W. G. Choe for helpful discussions. This work was supported by the Creative Research Initiatives of the Korean Ministry of Science and Technology.

[1] H.G. Schuster, *Deterministic Chaos: An Introduction* (VCH, Weinheim, 1995).
[2] P. Bak, Phys. Today **39**(12), 38 (1986).
[3] P. Coullet and K. Emilsson, Physica D **61**, 119 (1992).
[4] O. Steinbock, V. Zykov, and S. Müller, Nature (London) **366**, 322 (1993).
[5] V. Petrov, Q. Quyang, and H.L. Swinney, Nature (London) **388**, 655 (1997).
[6] A.L. Lin, M. Bertram, K. Martinez, H.L. Swinney, A. Ardelea, and G.F. Carey, Phys. Rev. Lett. **84**, 4240 (2000).
[7] A.L. Lin, A. Hagberg, A. Ardelea, M. Bertram, H.L. Swinney, and E. Meron, Phys. Rev. E **62**, 3790 (2000).
[8] H.-K. Park, Phys. Rev. Lett. **86**, 1130 (2001).
[9] C. Elphick, A. Hagberg, and E. Meron, Phys. Rev. E **59**, 5285 (1999).
[10] V.K. Vanag, L. Yang, M. Dolnik, A.M. Zhabotinsky, and I.R. Epstein, Nature (London) **406**, 389 (2000).
[11] J. Kim, J. Lee, and B. Kahng, Phys. Rev. E **65**, 046208 (2002).
[12] C. Elphick, A. Hagberg, and E. Meron, Phys. Rev. Lett. **80**, 5007 (1998).
[13] K.J. Lee, W.D. McCormick, Q. Ouyang, and H.L. Swinney, Science **261**, 192 (1994).
[14] K.J. Lee and H.L. Swinney, Phys. Rev. E **51**, 1899 (1995).
[15] A. Hagberg and E. Meron, Phys. Rev. Lett. **72**, 2494 (1994).
[16] K. Kaneko, *Theory and Applications of Coupled Map Lattices* (Wiley, New York, 1993).
[17] O. Rudzick and A. Pikovsky, Phys. Rev. E **54**, 5107 (1996).
[18] F.H. Willeboordse, Phys. Rev. E **65**, 026202 (2002).
[19] A. Goryachev and R. Kapral, Phys. Rev. Lett. **76**, 1619 (1996).
[20] A. Goryachev, R. Kapral, and H. Chaté, Int. J. Bifurcation Chaos Appl. Sci. Eng. **10**, 1537 (2000).
[21] J.-S. Park and K.J. Lee, Phys. Rev. Lett. **83**, 5393 (1999).
[22] J.-S. Park and K.J. Lee, Phys. Rev. Lett. **88**, 224501 (2002).
[23] D.P. Tse, A.M. Rucklidge, R.B. Hoyle, and M. Silber, Physica D **146**, 367 (2000).
[24] H.K. Ko, J. Lee, and K.J. Lee, Phys. Rev. E **65**, 056222 (2002).
[25] In this study, the source-sink transition is determined by the sign of the radial phase velocity. When it is judged by the sign of the group velocity as in Refs. [28,29], all spiral waves discussed in this paper are a source.
[26] V.K. Vanag and I.R. Epstein, Science **294**, 835 (2001).
[27] V.K. Vanag and I.R. Epstein, Phys. Rev. Lett. **88**, 088303 (2002).
[28] I.S. Aranson and L. Kramer, Rev. Mod. Phys. **74**, 99 (2002).
[29] Y. Gong and D.J. Christini, Phys. Rev. Lett. **90**, 088302 (2003).